required to produce an existing phase-shifter design at high volume. These figures indicate the distribution of cost and include attrition, burden, and profit. The attrition rates assumed were 10 percent on metal parts, 30 percent on ceramic parts, and a 4-percent rejection rate of completed assemblies at the final inspection level. The costs of materials are based on current prices on actual vendor quotations. Fabrication and assembly use known and proven techniques. Consequently, the figures of Table I are considered to be conservative with regard to ultimate high-volume production cost of an X-band dual-mode phase shifter.

CONCLUSIONS

A substantial body of knowledge exists about the design and manufacturing considerations for the dual-mode reciprocal latching ferrite phase shifter. Fundamental design techniques are well established for providing reasonable performance over moderately wide frequency bands. The weight–insertion loss tradeoff has been explored analytically and found to predict an optimum choice of material for low RF power applications. Parameters affecting switching and, in particular, shorted-turn damping, have been identified and expressed in normalized form for convenience. Finally, the manufacturing problem has been worked in far greater detail than the scope of this paper allows, to the conclusion that lightweight X-band phase shifters can be produced at high-volume rates for unit cost levels on the order of $10.00.

REFERENCES

[1] W. E. Hord, C. R. Boyd, Jr., and F. J. Rosenbaum, "Application of reciprocal latching ferrite phase shifters to lightweight electronic scanned phased arrays," *Proc. IEEE (Special Issue on Electronic Scanning)*, vol. 56, pp. 1931–1939, Nov. 1968.
[2] C. R. Boyd, Jr., "A dual-mode latching reciprocal ferrite phase shifter," *IEEE Trans. Microwave Theory Tech. (1970 Symposium Issue)*, vol. MTT-18, pp. 1119–1124, Dec. 1970.
[3] R. G. Roberts, "An X-band reciprocal latching Faraday rotator phase shifter," in *1970 IEEE G-MTT Int. Symp. Dig.*, May 1970, pp. 341–345.
[4] J. J. Green and F. Sandy, "Microwave properties of partially magnetized ferrites," Rome Air Development Center, Rome, N. Y., Final Rep. RADC-TR-69-338, Sept. 1969.

Computer Analysis of Microwave Propagation in a Ferrite Loaded Circular Waveguide—Optimization of Phase-Shifter Longitudinal Field Sections

A. M. DUPUTZ AND A. C. PRIOU, MEMBER, IEEE

***Abstract*—A theoretical analysis of the microwave propagation in a circular TE_{11} waveguide partially or completely loaded with an axially magnetized ferrite rod is presented. This study is based upon an exact analytical treatment of the Maxwell's equations, together with an original numerical method of solving transcendental equations with a complex variable. The introduction of the complex propagation constant $\Gamma = \alpha + j\beta$, taking in account the losses in the filling medium, had never been attempted because of the mathematical difficulties involved making essential the use of a large capacity computer. The developed program not only supplies all the propagation characteristics for a given structure but also enables us to optimize a phase-shift section in accordance with the user's requirements.**

This study is a first step towards the theoretical optimization of two types of reciprocal phasers: the dual mode phaser (DMP) and the polarization insensitive phaser (PIP), both widely used in array antenna systems. The computed results obtained for the basic section of such phasers operating at a central frequency of 9.5 GHz are given.

Obviously, this work is still incomplete since it does not include the optimization of all the components of a practical phase shifter, for example, the polarizers. Moreover, we have assumed the ferrite partially magnetized by a continuously variable bias field, although the PIP and the DMP are normally operated in a latching configuration; we presently complete our study according to these practical considerations.

Manuscript received September 5, 1973; revised January 4, 1974. This work was supported by the Direction des Recherches et Moyens d'Essais, the French Army Ministry.

The authors are with the Department d'Etudes et de Recherches en Micro-Ondes, Centre d'Etudes et de Recherches de Toulouse, Complex Aerospatial, Toulouse, France.

NOMENCLATURE

$$\beta_0^2 = \omega^2\epsilon_0\mu_0, \quad \lambda_0 = 2\pi/\beta_0, \quad \eta_0 = \left[\frac{\mu_0}{\epsilon_0}\right]^{1/2}$$

$$k_d^2 = \beta_0^2\epsilon_d\mu_d + \Gamma^2 \qquad k_{d'}^2 = \beta_0^2\epsilon_d\mu_d + \Gamma'^2$$

$$k_f^2 = \beta_0^2\epsilon_f\mu + \Gamma^2 \qquad k_{f'}^2 = \beta_0^2\epsilon_f\mu_i + \Gamma'^2$$

$$\bar{k}_f^2 = \epsilon_f\mu + \bar{\Gamma}^2, \quad \bar{k}_d^2 = \epsilon_d\mu_d + \bar{\Gamma}^2, \quad \bar{\Gamma}^2 = \Gamma^2/\beta_0^2$$

$$d = \frac{\mu_z k_f^2}{\mu}, \quad e = \frac{-K\Gamma\omega\epsilon_0\epsilon_f}{\mu}, \quad f = k_f^2 - \frac{\beta_0^2\epsilon_f K^2}{\mu}$$

$$g = \frac{K\Gamma\omega\mu_0\mu_z}{\mu}$$

$$S = \frac{\Gamma^i}{b}\left(\frac{1}{k_d{}^{i2}} - \frac{1}{k_f{}^{i2}}\right), \quad N = \frac{\beta_0^2\eta_0}{k_d}, \quad R = \frac{\beta_0^2\epsilon_d}{\eta_0 k_d}$$

$$U_f = \frac{\eta_0\mu_i}{k_f{}^i}, \quad U_d = \frac{\eta_0\mu_d}{k_d{}^i}, \quad V_f = \frac{\epsilon_f}{\eta_0 k_f{}^i}, \quad V_d = \frac{\epsilon_d}{\eta_0 k_d{}^i}$$

$$L_{1,2} = \frac{s_{1,2}}{\epsilon_f^2K^2 - \bar{k}_f^4}\left[\eta_0(\epsilon_f K^2 - \mu_f\bar{k}_f^2)\tau_{1,2} - \epsilon_f K\bar{\Gamma}\right]$$

$$M_{1,2} = \frac{\bar{\Gamma}}{b}\left[\frac{\bar{k}_f^2 - \eta_0 K\tau_{1,2}\bar{\Gamma}}{\epsilon_f^2K^2 - \bar{k}_f^4} + \frac{1}{\bar{k}_d^2}\right]$$

$$P_{1,2} = \frac{\epsilon_f s_{1,2}}{\epsilon_f K^2 - \bar{k}_f^4}\left[\frac{\bar{k}_f^2}{\eta_0} - K\bar{\Gamma}\tau_{1,2}\right]$$

$$Q_{1,2} = \frac{1}{b}\left\{\frac{\bar{\Gamma}\bar{k}_f^2\tau_{1,2} - \epsilon_f{}^{2K}/\eta_0}{\epsilon_f{}^2k^2 - \bar{k}_f^4} + \frac{\bar{\Gamma}\tau_{1,2}}{\bar{k}_d^2}\right\}$$

$$W_{1,2} = \{\eta_0[\epsilon_f k^2 - \mu\bar{k}_f^2]\tau_{1,2} - \bar{\Gamma}\epsilon_f k\}s_{1,2}J_1'(s_{1,2}a) - n\frac{\eta_0 K\bar{\Gamma}^2}{a}\tau_{1,2}J_1(s_{1,2}a).$$

I. INTRODUCTION

THE most commonly used method of calculating the electromagnetic wave propagation in loaded waveguides consists of writing out the Maxwell's equations in the filling media together with the boundary conditions for the electromagnetic (EM) fields on the interface of these media and on the guide wall. From this, we deduce the characteristic equation which provides the mode spectrum. Each mode is thus defined by its propagation constant $\Gamma = \alpha + j\beta$. It is then easy to complete the study by determining the EM fields and the power they carry.

Such a method is well known [1]–[3] and can be applied straightforwardly to the structure under study: a TE_{11} circular waveguide loaded with an axially magnetized ferrite rod and a dielectric tube. As the guide wall (a perfect conductor) and the ferrite–dielectric interface coincide with the θ coordinate surfaces (in cylindrical polar coordinates r,θ,z), it is relatively easy to obtain an exact analytical derivation of the characteristic equations which is rarely the case in the study of waves guided in anisotropic and inhomogeneous media. These equations include Bessel functions of complex argument. In order to solve them, we have developed a general method of searching for the zeros of a transcendental function $F(\Gamma)$ by means of a computer program.

We have thus worked out a general technique which, starting from the physical and geometrical specifications of a structure, supplies all the information desired for each propagating mode, and particularly the precise characterization of the fundamental mode (mode of weakest attenuation). A program of this type may be very useful for the engineer who wants to know rapidly and exactly the microwave behavior of a given configuration.

A Faraday rotation phase shifter generally consists of a phase-shift section located between two circular polarizers. In this study we only deal with the phase-shift section of two reciprocal phasers of this class: the polarization insensitive phaser (PIP) and the dual mode phaser (DMP). The optimization of the basic section of these phasers involves the choice of the filling materials and the determination of the optimum geometry.

This paper begins with a review of the mathematical derivation of the characteristic equations for the two basic structures: the ferrite filled guide and the guide loaded with a ferrite rod axially located and surrounded by dielectric. Then, we briefly review the numerical method for solving the equations $F(\Gamma) = 0$, this having formed the subject of a previous publication [4]. We also give the analytical expressions of the field components, Poynting vector, and absorbed power.

The second part of this work is devoted to the theoretical optimization of DMP and PIP centered at the frequency 9.5 GHz. We analyze the results supplied by our computer program. The use of normalized parameters versus frequency makes possible a limited scaling to other frequency regions.

II. MODAL ANALYSIS OF THE TWO BASIC STRUCTURES EXCITED BY THE CIRCULARLY POLARIZED TE_{11} MODES

A. Geometrical Definition—Physical Parameters

A circular waveguide of infinite length and radius "a" contains on its axis a ferrite rod of radius "b" surrounded by dielectric [Fig. 1(b)]. The DMP generally consists of a metallized ferrite rod, i.e., $b = a$ [Fig. 1(a)]. The ferrite rod is axially magnetized by an uniform dc magnetic field. We assume that the internal field H_i is equal to the applied field H_a.

The ferrite and dielectric materials are characterized at the angular frequency ω by their relative permittivity and permeability given by

$$\epsilon_d = \epsilon_d'(1 - j\tan\delta_d) \qquad \mu_d = 1$$

for the dielectric and

$$\epsilon_f = \epsilon_f'(1 - j\tan\delta_f) \qquad \mu = \begin{vmatrix} \mu & -jK & 0 \\ jK & \mu & 0 \\ 0 & 0 & \mu_z \end{vmatrix}$$

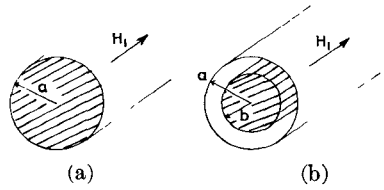

(a) (b)

Fig. 1. (a) Ferrite fully filled circular waveguide. (b) Inhomogeneously loaded circular waveguide.

for the ferrite, where

$$\mu = \mu' - j\mu'', \quad \mu_z = \mu_z' = j\mu_z'', \quad K = K' - jK''.$$

For the demagnetized ferrite ($H_i = 0$)

$$\mu = \mu_z = \mu_i = \mu_i' - j\mu_i'' \qquad \text{and} \qquad K = 0.$$

The elements μ, K, and μ_z of the permeability tensor depend upon the magnetization state of the ferrite.

B. Coupled Wave Equations—Hybrid Modes

Writing out the Maxwell's equations in each filling medium of the guide generates wave equations in terms of the longitudinal components of E and H fields.

We obtain in the isotropic dielectric a wave equation of the classical type:

$$(\nabla_T^2 + k_d^2)\begin{Bmatrix} E_{zd} \\ H_{zd} \end{Bmatrix} = 0 \tag{1}$$

and, in the ferrite, two coupled wave equations linking E_{zf} and H_{zf}:

$$(\nabla_T^2 + d)H_{zf} + eE_{zf} = 0 \tag{2}$$

$$(\nabla_T^2 + f)E_{zf} + gH_{zf} = 0. \tag{3}$$

If e and g are nonzero, (2) and (3) imply the existence of hybrid modes with six field components. Now, e and g can be zero in only two cases as follows.

1) If $K = 0$, the ferrite is demagnetized and then equivalent to an isotropic dielectric with scalar constants ϵ_f, μ_i.

2) If $\Gamma = 0$, there is no propagation along the z direction ($e^{-\Gamma z} = 1$). This can be considered as a cutoff due to the medium. We shall exclude this case from our study.

Let us first of all examine the case of the magnetized ferrite when the dc field and the traveling wave have the same direction (i.e., $H_i > 0$). The coupled wave equations can be solved by using an algebraic method close to that of Kales [1] (see Appendix I).

The general expressions of the complex longitudinal components are of the following form:

$$[\gamma_1 J_n(s_1 r) + \gamma_2 J_n(s_2 r)] \exp(jn\theta) \exp(-\Gamma z),$$

in the ferrite

$$[\gamma_2' J_n(k_d r) + \gamma_2' Y_n(k_d r)] \exp(jn\theta) \exp(-\Gamma z),$$

in the dielectric

$\gamma_1, \gamma_2, \gamma_1', \gamma_2'$: integration constants

J_n, Y_n: Bessel functions of first and second kind.

The incident wave being the TE_{11} mode of the empty guide, we obtain $n = +1$ for a left-hand (or negative) circular polarization and $n = -1$ for the right-hand (or positive) circular polarization. It should be remembered that the polarization of a guided wave is, by definition, that of the transverse fields on the waveguide axis.

Each of the polarizations is propagated in the circular guide independently of one another. They are the normal modes of the structure. They are degenerate when the guide is filled with an isotropic medium, whether homogeneous or not. But the anisotropy induced by magnetizing the ferrite removes this degeneracy. The two normal modes with positive and negative circular polarizations travel with different propagation constants, thus with different radial wavenumbers s. Consequently, the exponential dependence in θ cannot be reduced to a cosine function, thus to an amplitude factor. It occurs as a phase factor just like $\exp(-j\beta z)$ and $\exp(j\omega t)$.

Thus the factor of the real field components should be written: $\cos(\omega t - \beta z \pm \theta)$, which corresponds to a progressive wave along both the z axis and the θ azimuth. We call rotative modes the modes that present this peculiarity. We shall point out that the negative rotative mode corresponds to a left-hand circularly polarized wave, and the positive rotative mode corresponds to a right-hand polarized wave.

Let us now consider the case of the demagnetized ferrite ($H_i = 0$). As the wave equations in the ferrite are no longer coupled, the preceding treatment is not applicable.

The wave equation in the isotropic ferrite is as follows:

$$(\nabla_T^2 + k_{fi}^2)\begin{matrix}(E_{zf}) \\ (H_{zf})\end{matrix} = 0. \tag{4}$$

However, the modes preserve in this case a hybrid structure if the waveguide contains two media or more, because the six field components are necessary in order to satisfy the boundary conditions on the interface of the media.

In Appendix II, we give the expressions of the field components in both media: ferrite and dielectric, and in both cases: $H_i > 0$ and $H_i = 0$.

C. Boundary Conditions—Characteristic Equations

The simplest case is that of the ferrite filled waveguide since there are only two boundary conditions, i.e., the tangential components of the electric field are zero on the guide wall.

In the case of the guide with heterogeneous filling, the tangential electric and magnetic fields must be continuous on the ferrite–dielectric interface, which adds a further four equations.

The characteristic equation of the propagation is obtained by setting equal to zero the determinant of the

system of the boundary conditions equations: we give successively the characteristic equations of the filled guide (5) and of the partly filled guide (6). For each of these structures, there are two cases to consider: the first is that of the demagnetized ferrite ($H_i = 0$) for which the positive and negative rotative modes correspond to the same characteristic equation [(5a) and (6a)]; and the second is that of the magnetized ferrite ($H_i > 0$) where each rotative mode corresponds to a different characteristic equation [(5b) and (6b)]. In the latter case, we only write one equation for the two modes and it is the value of the azimuthal wavenumber which enables us to distinguish one from another.

Characteristic equations for the filled guide are the following.

1) $H_i = 0$. It is the trivial case:

$$F(\Gamma^i) = J_1'(k_f{}^i a) = 0, \quad \text{for the TE modes}$$

$$F(\Gamma^i) = J_1(k_f{}^i a) = 0, \quad \text{for the TM modes.} \tag{5a}$$

2) $H_i > 0$:

$$F(\Gamma) = W_2 J_1(s_1 a) - W_1 J_1(s_2 a) = 0. \tag{5b}$$

With characteristic equations for the partly filled guide, we have found the determinantal form more convenient for the numerical treatment.

D. Numerical Analysis of the $F(\Gamma) = 0$ Equations

Once we have established the analytical expression of the $F(\Gamma)$ functions, we can carry out the search of all the roots in the Γ complex plane in order to determine the mode spectrum. We are going to review here the principle of the computation method developed in our laboratory [4].

First we choose a closed contour in the Γ plane capable of including all the modes which can be propagated. Excluding *a priori* the half-plane $\alpha < 0$ which would not correspond to a physical solution, and the $\beta < 0$ zone associated with backward modes, we define a rectangle in the remaining quadrant ($\alpha > 0, \beta > 0$) by fixing a maximum value for α and β, respectively. In our case α maximum is equal to a few tens of decibels per centimeter, a value above which the mode is so strongly attenuated that it presents no practical interest; β maximum is a sufficiently high value from which $F(\Gamma)$ becomes infinite.

The number of modes which can be propagated (and which satisfy the above criteria) is given by the number of zeros of $F(\Gamma)$ contained in the rectangle thus defined.

1) Determination of the Number of Zeros of $F(\Gamma)$: This is based on a well-known theorem: the number N of zeros of an analytical and holomorphous function $F(\Gamma)$ that are contained within a contour C of the complex plane Γ is given by:

1) $H_i = 0$:

$$\begin{vmatrix}
0 & 0 & J_1(k_d{}^i a) & Y_1(k_d{}^i a) & 0 & 0 \\
0 & 0 & 0 & 0 & J_1'(k_d{}^i a) & Y_1'(k_d{}^i a) \\
J_1(k_f{}^i b) & 0 & -J_1(k_d{}^i b) & -Y_1(k_d{}^i b) & 0 & 0 \\
0 & J_1(k_f{}^i b) & 0 & 0 & -J_1(k_d{}^i b) & -Y_1(k_d{}^i b) \\
nSJ_1(k_f{}^i b) & U_f J_1'(k_f{}^i b) & 0 & 0 & -U_d J_1'(k_d{}^i b) & -U_d Y_1'(k_d{}^i b) \\
V_f J_1'(k_f{}^i b) & -nSJ_1(k_f{}^i b) & -V_d J_1'(k_d{}^i b) & -V_d Y_1'(k_d{}^i b) & 0 & 0
\end{vmatrix} = 0. \tag{6a}$$

2) $H_i > 0$:

$$\begin{vmatrix}
0 & 0 & J_1(k_d a) & Y_1(k_d a) & 0 & 0 \\
0 & 0 & 0 & 0 & J_1'(k_d a) & Y_1'(k_d a) \\
J_1(s_1 b) & J_1(s_2 b) & -J_1(k_d b) & -Y_1(k_d b) & 0 & 0 \\
\tau_1 J_1(s_1 b) & \tau_2 J_1(s_2 b) & 0 & 0 & -J_1(k_d b) & Y_1(k_d b) \\
L_1 J_1'(s_1 b) + nM_1 J_1(s_1 b) & L_2 J_1'(s_2 b) + nM_2 J_1(s_2 b) & 0 & 0 & -NJ_1'(k_d b) & -NY_1'(k_d b) \\
P_1 J_1'(s_1 b) + nQ_1 J_1(s_1 b) & P_2 J_1'(s_2 b) + nQ_2 J_1(s_2 b) & RJ_1'(k_d b) & RY_1'(k_d b) & 0 & 0
\end{vmatrix} = 0. \tag{6b}$$

$$N = \frac{1}{2\pi j} \oint_C \frac{F'(\Gamma)}{F(\Gamma)} d\Gamma \tag{7}$$

provided that no zero belongs to C. The numerical evaluation of this integral for a large number of points along C would be rather time consuming.

The number N can, however, be evaluated much more simply by considering the phase of the function $F(\Gamma)$ along the contour where each 2π jump corresponds to a zero within the contour. In fact, in developing the preceding relation, we have

$$\oint_C \frac{F'(\Gamma)}{F(\Gamma)} d\Gamma = \log F(\Gamma)]_C = \log F(\Gamma)]_C + j \arg F(\Gamma)]_C \tag{8}$$

then

$$N = \frac{\arg F(\Gamma)}{2\pi}\Big]_C. \tag{9}$$

From the numerical point of view, the $F(\Gamma)$ phase is defined between $-\pi$ and $+\pi$. All that is needed is to detect the rough phase shifts from $-\pi$ to $+\pi$ or from $+\pi$ to $-\pi$ by following the contour in a clockwise way, and count $+1$ at each jump from $-\pi$ to $+\pi$ and -1 at each reverse jump. The sum so obtained gives the number of zeros inside the countour, a zero being itself a phase shift from π to 0, or from $-(\pi/2)$ to $+\pi/2$ for instance, as we can see on Fig. 2 where we count three zeros.

If the function $F(\Gamma)$ is not holomorphous, as it occurs in the case of the circular waveguide, the sum obtained is equal to the difference $(N - P)$ of the number of zeros and of the number of poles located within C. But it is easy to return to the preceding case, as we know the values of Γ corresponding to these poles:

$$\Gamma_{\text{critic}} = [-\beta_0^2 \epsilon_f (\mu \pm K)]1/2.$$

2) Localization of the Zeros of $F(\Gamma)$: Starting from the positions on the contour of the phase jumps of $F(\Gamma)$ we can look for the exact value of the zeros by using the method proposed by Gardiol [5]. This consists of following the equiphases of $F(\Gamma)$ for which we have registered a jump of $-\pi$ to $+\pi$ by directing towards the decreasing amplitudes up to the close neighborhood of the desired root. The exact position of the root is then determined by the Newton–Raphson interpolation method.

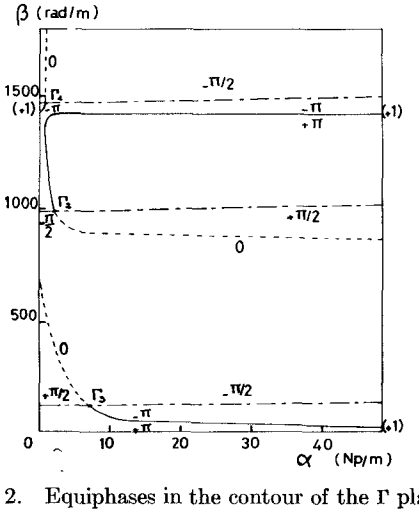

Fig. 2. Equiphases in the contour of the Γ plane.

E. Calculation of the Fields and Powers

We must consider the propagation of a single mode if we wish to relate the magnitude of the fields in the structure to the level of the incident power P_i. Thus we choose the fundamental mode and normalize the fields by putting: $P_i = \lambda_0^2$ W, where λ_0 is the free space wavelength expressed in meters.

The average incident power flow can be calculated in the section $z = 0$ chosen arbitrarily as an input section. We have

$$P_i = R_e \frac{1}{2} \int_{S(z=0)} (\boldsymbol{E}_T \times \boldsymbol{H}_T^*) \cdot \boldsymbol{z}\, ds.$$

At every point (r,θ,z) in the section, the real part of the longitudinal component of the complex Poynting vector represents the average power flow per unit surface around the point under consideration. This flow only depends upon r in a given section, that is

$$P(r) = \text{Re}\left[\frac{(\boldsymbol{E}_T \times \boldsymbol{H}_T^*) \cdot \boldsymbol{z}}{2}\right]$$

$$= \tfrac{1}{2} \text{Re}\,[E_r(r) H_\theta^*(r) - E_\theta(r) H_r^*(r)].$$

The $P(r)$ curves thus express the radial distribution of the average power flow.

Starting from the general expression of the volume density of average power absorbed in an homogeneous medium propagating an harmonic wave

$$p_a = \tfrac{1}{2} \text{Re}\,\{ j\omega\epsilon_0[\boldsymbol{E}^* \in \boldsymbol{E} + \boldsymbol{H}^* \mu \boldsymbol{H}]\}.$$

We can calculate the average power absorbed by each material along the unit length of the guide taken between $z = 0$ and $z = 1m$. We obtain in the dielectric

$$P_{ad} = \frac{\pi\omega}{2\alpha} [1 - \exp(-2\alpha)]\epsilon_0\epsilon_d' \tan\delta_d \int_b^a |\, \boldsymbol{E}_d(r)\,|^2 r\, dr$$

and in the ferrite,

$$P_{af} = \frac{\pi\omega}{2\alpha} [1 - \exp(-2\alpha)][\epsilon_0\epsilon_f' \tan\delta_f \int_0^b |\, \boldsymbol{E}_f(r)\,|^2 r\, dr$$

$$+ \mu_0\mu_z'' \int_0^b |\, H_{zf}(r)\,|^2 r\, dr + \mu_0\mu'' \int_0^b |\, \boldsymbol{H}_{Tf}(r)\,|^2 r\, dr$$

$$+ j\mu_0 K'' \int_0^b (H_{rf}(r) H_{\theta f}^*(r) - H_{\theta f}(r) H_{rf}^*(r)) r\, dr].$$

This study of the normal modes of both basic structures has enabled us to characterize completely the propagation of a circularly polarized wave when the magnetic field is applied along the direction of propagation. By considering

the characteristic equations, we can see that a reversal of the propagation direction is equivalent to a reversal of the magnetization direction. Only the rotation sense of the field configuration with respect to the sense of the applied magnetic field is relevant. It follows that a reciprocal system can be obtained by cascading in tandem two basic structures of the same length magnetized in opposite directions, or else magnetized in the same direction but separated by a polarization inverter (half-wave plate) [Fig. 2(b)]. This is the operating principle of a transmission type PIP [6] that we are now going to examine in closer detail.

III. OPERATING PRINCIPLE OF A TRANSMISSION PIP

A. Excitation of a Circularly Polarized TE_{11} Wave

The ferrite is partially magnetized and the bias field level is below the knee of the magnetization curve of the material. If β^+ and β^- are the phase constants, respectively, of right- and left-hand circular polarization, we have in this zone

$$\beta^+ < \beta^i < \beta^-$$

$\phi^i = \beta^i l$, initial phase taken as reference

$\phi^+ = \beta^+ l$

$\phi^- = \beta^- l$.

Where l is the length of each section, the relative phase shifts resulting from the application of the dc field are

$$\Delta\phi^+ = \phi^+ - \phi^i < 0, \quad \text{phase advance}$$

$$\Delta\phi^- = \phi^- - \phi^i > 0, \quad \text{phase delay.}$$

Regardless of the sense of rotation of the input wave, it undergoes a total phase shift:

$$\Delta\phi = \Delta\phi^+ + \Delta\phi^- = [\beta^+ + \beta^- - 2\beta^i]l$$

$$A = (\alpha^+ + \alpha^-)l.$$

B. Excitation by a Linearly Polarized TE_{11} Wave

Any linearly polarized wave can be constructed from the counter-rotating circularly polarized waves.

After traveling through the first section ($z = l$), the complex electric field can be written

$$\boldsymbol{E}(r,\theta,l) = \boldsymbol{E}^+(r) \exp(-j\theta) \exp(-\Gamma^+ l) + \boldsymbol{E}^-(r) \exp(+j\theta) \exp(-\Gamma^- l)$$

and, at the ouput of the second section ($z = 2l$), it becomes

$$\boldsymbol{E}(r,\theta,2l) = \boldsymbol{E}^+(r) \exp(-j\theta) \exp[-(\Gamma^+ + \Gamma^-)l] + \boldsymbol{E}^-(r) \exp(+j\theta) \exp[-(\Gamma^+ + \Gamma^-)l].$$

The wave transmitted by the PIP has thus undergone the attenuation $A = (\alpha^+ + \alpha^-)l$ and its phase has varied from $\phi = (\beta^+ + \beta^-)l$. Taking as a reference the phase at zero bias field, the phase shift is equal to

$$\Delta\phi = (\beta^+ - \beta^i)l + (\beta^- - \beta^i)l = (\beta^+ + \beta^- - 2\beta^i)l.$$

We thus verify that the phase and attenuation characteristics of such a phaser do not depend upon the nature of the input polarization. Furthermore, the electric field preserves its initial polarization direction.

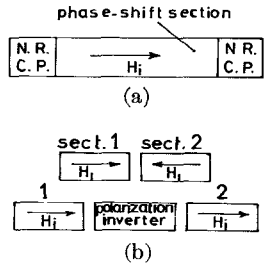

Fig. 3. (a) DMP. (b) Two versions of the transmission polarization insensitive phaser.

IV. OPERATING PRINCIPLE OF A DMP

The DMP [7] is particularly simple in concept. A metallized ferrite cylinder fulfills both the polarization and phase-shift functions by means of proper magnetization techniques [Fig. 3(a)]. The central part is axially magnetized by a solenoid (phase-shift section), whereas the input and output sections are biased by a transverse quadrupole magnetic field, each of which constitutes a nonreciprocal circular polarizer [8].

The incidental TE_{11} wave with linear polarization is transformed into a hybrid wave with circular polarization, the sense of this polarization depending upon the wave propagation sense through the input polarizer. At the output, we find a wave with the same structure as the input wave. This system is obviously reciprocal since, in the phase-shift section, the sense of rotation of the field configuration with respect to the magnetization direction remains the same for both propagation directions.

V. THEORETICAL OPTIMIZATION OF THE TWO PHASERS

A. Purposes of the Optimization

The aim of this study of optimization is to define a structure propagating only the fundamental mode, and providing a maximal phase shift per unit length for minimal insertion loss. So we are seeking to determine the geometry of the structure, and the filling materials such as the "figure of merit," $m = (\Delta\beta \text{ max})/(\alpha \text{ max})$ defined within a certain range of the dc field, is maximal.

The optimization of the DMP involves the choice of the ferrite material and the guide radius. For the optimization of the PIP we shall keep the same ferrite and the same guide radius, and shall look for the best dielectric to use with it, as well as the optimum filling factor b/a.

B. Characterization of the Studied Materials

The "Lignes Télégraphiques et Téléphoniques" Company has given us the microwave characteristics of a

TABLE I

FERRITES								DI-ELECTRICS		
Type	Composition	4 Π Ms (G)	Δ H (Oe)	ε_f	tg δ_f	μ'_i	μ''_i	Composition	ε_d	tg δ_d
6101	NiZnCr	2 420	23	10,9	$0{,}5\times10^{-3}$	0,78	10^{-2}	SiO2	3,8	2×10^{-4}
6301	MgMn	2 030	3	12,6	$0{,}5\times10^{-3}$	0,77	$2{,}9\times10^{-3}$	BeO	6,4	4×10^{-4}
6301-1	MgMn	2 230	3,6	12,7	$0{,}3\times10^{-3}$	0,73	6×10^{-4}	Al_2O_3	9,4	5×10^{-4}
6301-2	MgMn	2 400	3,3	13,1	$0{,}2\times10^{-3}$	0,69	5×10^{-4}	TiO_{2-}		
6307	MgMnTiNa	1 790	7	13,7	$0{,}3\times10^{-3}$	0,82	$1{,}5\times10^{-3}$	2MgO	15	2×10^{-4}
								$BaTiO_9$	35	4×10^{-4}
								TiO_2	85	$4{,}5\times10^{-4}$

selection of available ferrite and dielectric materials (Table I), together with the initial magnetization curve of each ferrite.

At the present time, we do not know the exact dependence of the permeability tensor elements of each ferrite on the internal static field and the frequency. So, in order to describe the different states of magnetization of the ferrites under consideration, we have used the semi-empirical formulas proposed by Green [9] and Rado [10] for the real parts of μ,K, and μ_z:

$$\mu' = \mu_i' + (1 - \mu_i') \frac{\tan h[1.25(M/M_S)^2]}{\tan h 1.25}$$

$$\mu_z' = \mu_i'[1 - (M/M_S)^{5/2}]$$

$$K' = -\frac{\gamma M}{\omega}.$$

By referring to the same authors, we assume the following for the imaginary parts:

$$\mu'' = \mu_z'' = \text{constant} = \mu_i''$$

$$K'' = \text{constant} = 0.$$

Consequently, the computer results and curves which we present here, and principally those including the insertion loss, are not final. They are subject to correction once the nonsaturated ferrite permeability measurements currently being made in our laboratory are finished.

C. Results

We have fixed the frequency band at 9.3–9.7 GHz and the range of variation of the dc field at 0–50 Oe.

For both practical (to reduce the space required) and theoretical (to eliminate higher order modes propagation) reasons, we are considering guides with a radius less than the cutoff radius of the empty TE_{11} waveguide. Rather than the radius "a" of the guide, we introduce the normalized radius $a/\lambda_0 = af/c$ (f: frequency; c: velocity of light). The cutoff of the TE_{11} mode in the empty guide occurs for $a/\lambda_0 \simeq 0.293$. We have varied a/λ_0 from 0.124 to 0.285 which corresponds, for the central frequency of 9.5 GHz, to radii between 4 and 9 mm.

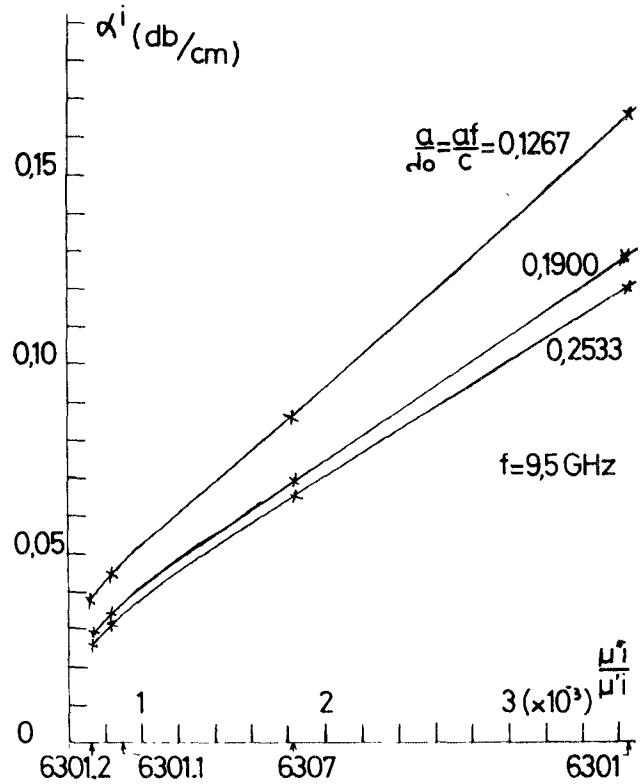

Fig. 4. Insertion losses in the demagnetized state for ferrite fully filled waveguides of different radius versus the loss tangent of some LTT ferrites.

Figs. 4–8 concern the ferrite filled guide and enable us to select the ferrite and the guide radius best adapted to the desired type of operation: a waveguide section excited by positive and negative circular polarizations (the case of the DMP) or two sections in tandem excited by a linear or a circular polarization (the case of the PIP). We note $\Delta\beta$,m when these terms refer to the PIP and $\Delta\beta^+$,m^+,$\Delta\beta^-$,m^- when they refer to the DMP. We notice (Fig. 4) that the initial attenuation ($H_i = 0$) of a circularly polarized wave increases quasi-linearly with the magnetic loss tangent μ_i''/μ_i' of the ferrites. The LTT 6301-2 ferrite is the least lossy and as a result of its high saturation magnetization ($4\Pi M_s = 2400$ G) and its weak μ_i'($\mu_i' = 0.69$) we can expect it to be the best choice for

making a phase shifter. On the other hand, the LTT 6101 ferrite characterized by high magnetic loss, can be excluded. We notice, moreover, that if the radius "a" is increased, the attenuation decreases; nevertheless, approaching the cutoff, the propagation of a second mode appears. We must therefore choose a normalized radius value a/λ_0 such that only the fundamental mode can be propagated and we shall limit our study to this mode.

Fig. 5 shows the effect of the radius "a" and of the frequency on the maximum relative phase shifts (phase shifts relative to the maximum value of the bias field H_i = 50 Oe) available with a guide filled with LTT 6301-2 ferrite for the three types of operation. The part of the curve which is traced with a dotted line corresponds to a maximum for $\Delta\beta$ obtained for an H_i value lower than 50 Oe. Beyond a radius of 8 mm ($a/\lambda_0 = 0.25$) at least two modes can be propagated. Figs. 6–8 represent variations in the figures of merit m^+,m^-,m versus a/λ_0 when the guide is filled successively with each of the ferrites. They confirm the choice of the 6301-2 ferrite.

Table II gives the optimal operating features of the phase-shift section using the guide filled with the LTT 6301-2 ferrite.

The analysis of the behavior of a guide loaded with a LTT 6301-2 ferrite rod surrounded by one of the proposed

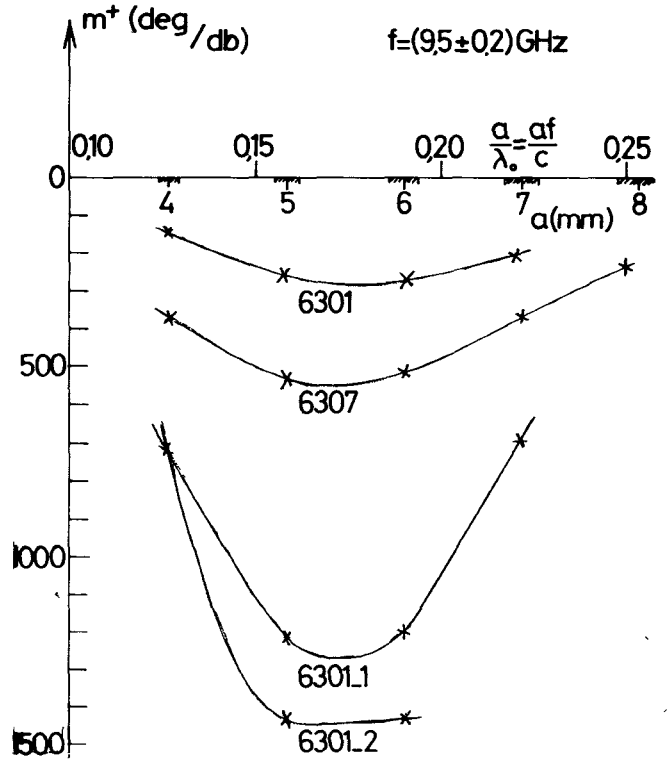

Fig. 6. Circularly polarized phaser using the fundamental positive rotative mode in a ferrite fully filled waveguide section.

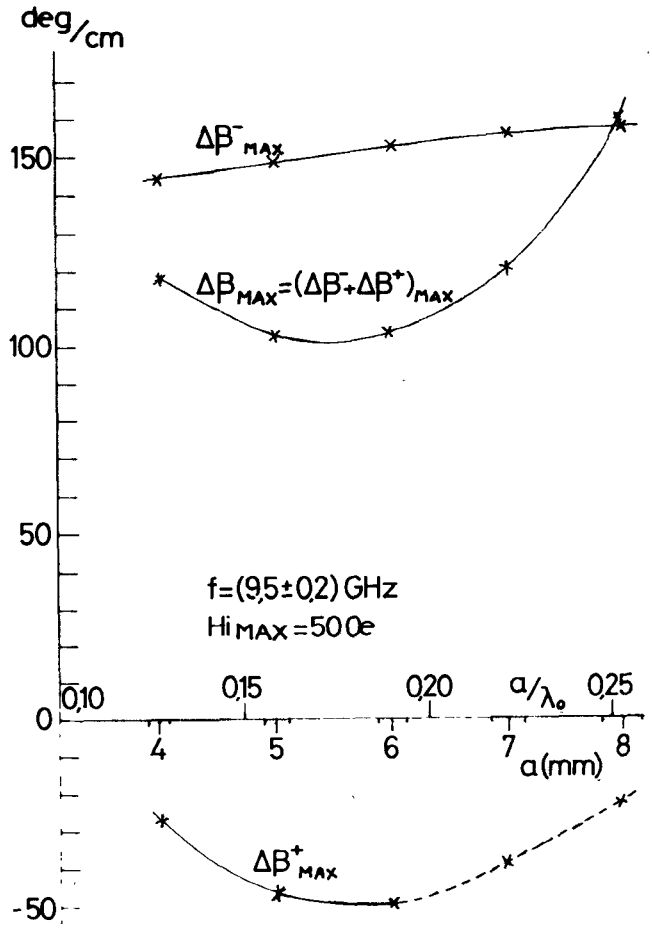

Fig. 5. Maximum relative phase shift for waveguides fully filled with the LTT 6301-2 ferrite.

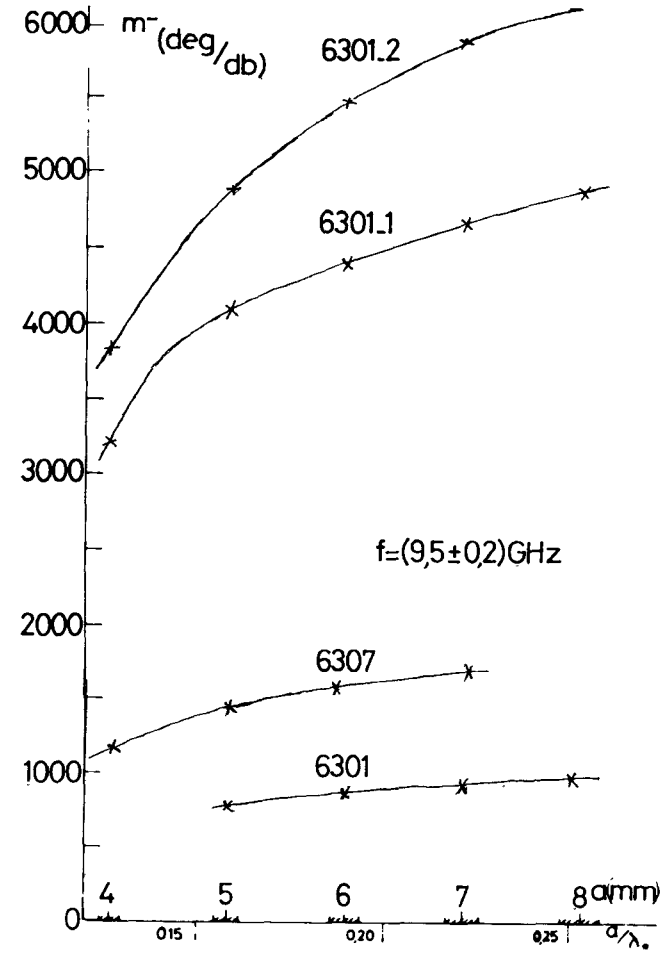

Fig. 7. Circularly polarized phaser using the fundamental negative rotative mode in a ferrite fully filled waveguide section.

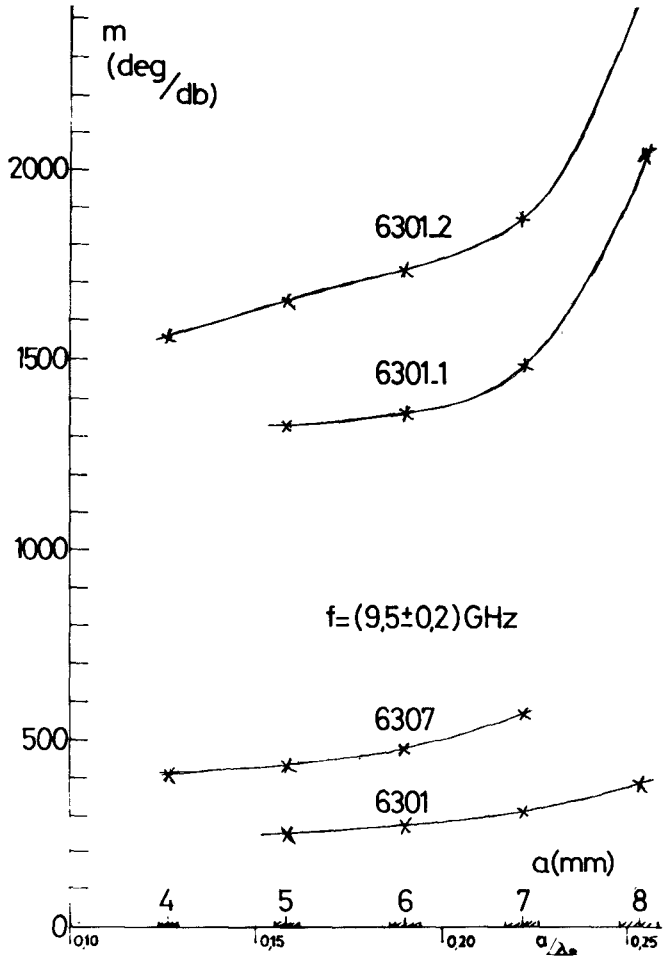

Fig. 8. Ferrite fully filled PIP element.

TABLE II

Type of Operation	Waveguide fully filled with L.T.T. 6301-2 ferrite - f = 9,5 GHz							
	a optimum (mm)	a/λ_0 (optimum)	$\Delta\beta$ max (deg/cm)	α max (db/cm)	m (deg/db)	length for $\Delta\beta$ max =360° (cm)	insertion losses (db)	dispersion (deg/GHz)
Positive mode	6	0,19	-49,5	0,034	1 440	7,27	0,247	2
Negative mode	8	0,25	+158,7	0,026	6 100	2,27	0,059	3
Transmission P.I.P.	8	0,25	+160,7	0,065	2 473	2,24x2=4,48	0,146	13

dielectrics leads to the following conclusions. When the radius "a" is greater than 6 mm, several higher order modes can be propagated even if we use the dielectric with the lowest permittivity (S_iO_2); for a radius of 6 mm, the dielectric must have a permittivity lower than that of the ferrite in order to propagate a single mode.

Figs. 9–11 allow us to determine, for a guide with a 6-mm radius the optimum filling factor when the 6301-2 ferrite is associated, respectively, with the three dielectrics of lowest permittivities (S_iO_2,B_eO,Al_2O_3). It is the fused silica with $\epsilon_d = 3.8$ which gives the best results for the three types of working.

Table III presents the optimal operating features of the phase-shift sections using a filled composite guide (LTT 6301-2 ferrite + S_iO_2).

VI. CONCLUSION

This study has enabled us to improve our knowledge of the microwave behavior of the PIP and DMP phase shifters, and so to establish analytically an optimization of the phase-shift section corresponding to each of these devices.

The mathematical difficulties that we have encountered during the numerical solving of the characteristic equations have led us to develop a computer program very general in scope which can be adapted to the search of

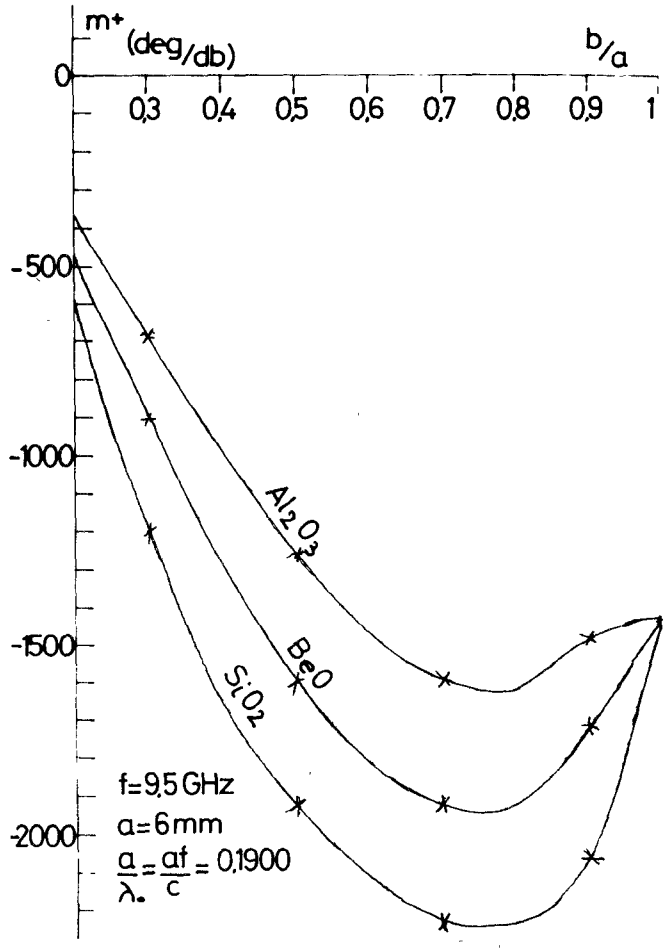

Fig. 9. Circularly polarized phaser using the fundamental positive rotative mode in a waveguide section containing an LTT 6301-2 ferrite rod surrounded by dielectric.

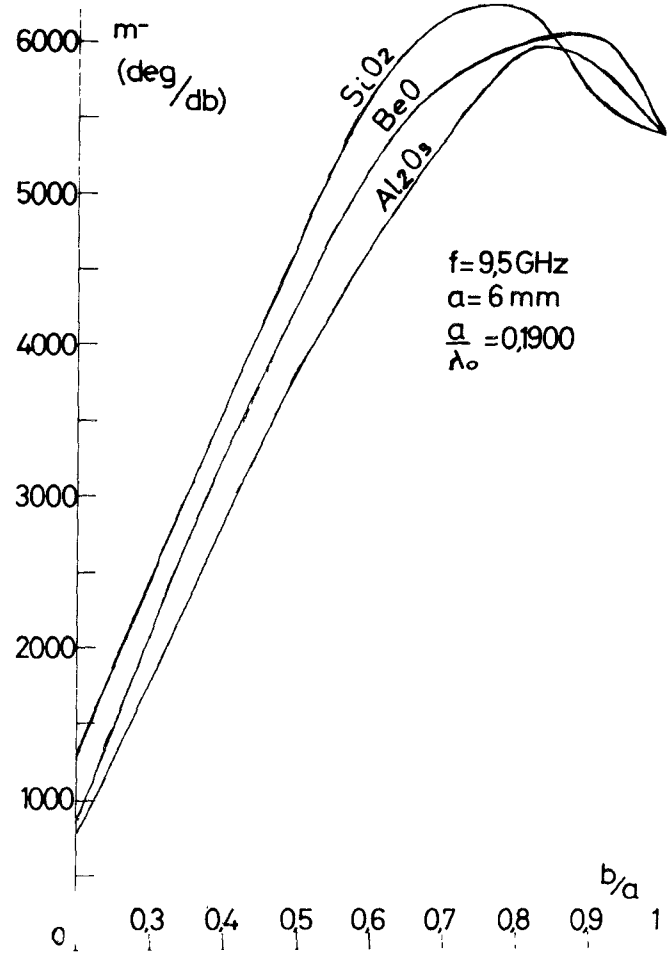

Fig. 10. Circularly polarized phaser using the fundamental negative rotative mode in a waveguide section containing an LTT 6301-2 ferrite rod surrounded by dielectric.

the complex roots of any analytical function, provided that these roots can be localized within a complex plane closed contour, and that any possible poles on the inside of the contour are known. In addition, we have generated numerical tables of the complex Bessel functions (order 0 and 1) and their derivatives, tables which, to our knowledge, were hitherto incomplete.

The theoretical investigations shall be extended now to the other components of the phasers, especially the nonreciprocal circular polarizer of the DMP.

Furthermore, by considering these devices from a more practical standpoint, we intend to analyze the behavior of the PIP and DMP operated at remanence, in order to define a latching figure of merit. Special effort shall be devoted to the temperature stabilization and broadbanding techniques.

APPENDIX I

SOLUTION OF THE COUPLED WAVE EQUATIONS SYSTEM

From (2) and (3), we can see that E_{zf} and H_{zf} satisfy separately a wave equation of the fourth order.

To obtain a second-order equation, we put

$$E_{zf} = \psi_1 + \psi_2$$

$$H_{zf} = \tau_1\psi_1 + \tau_2\psi_2, \qquad \text{with } \tau_1 \neq \tau_2 \tag{A-1}$$

ψ_1 and ψ_2 being two independent variables.

By introducing these expressions of E_{zf} and H_{zf} into (2) and (3), we obtain

$$\nabla_T^2\psi_1 + (f + g\tau_1)\psi_1 + \nabla_T^2\psi_2 + (f + g\tau_2)\psi_2 = 0$$

$$\tau_1\nabla_T^2\psi_1 + (e + d\tau_1)\psi_1 + \tau_2\nabla_T^2\psi_2 + (e + d\tau_2)\psi_2 = 0. \tag{A-2}$$

Suppose we can determine τ_1 and τ_2 as

$$f + g\tau_1 = s_1^2$$

$$f + g\tau_2 = s_2^2$$

and

$$e + d\tau_1 = \tau_1 s_1^2$$

$$e + d\tau_2 = \tau_2 s_2^2. \tag{A-3}$$

The relations (A-2) can thus be written

$$\nabla_T^2\psi_1 + s_1^2\psi_1 + \nabla_T^2\psi_2 + s_2^2\psi_2 = 0$$

$$\tau_1(\nabla_T^2\psi_1 + s_1^2\psi_1) + \tau_2(\nabla_T^2\psi_2 + s_2^2\psi_2) = 0.$$

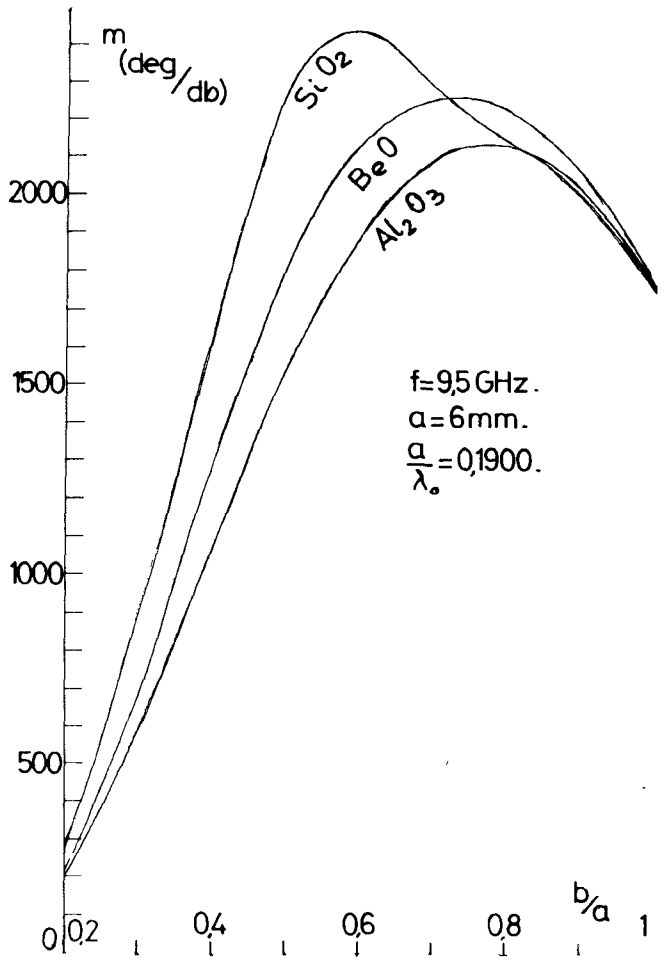

Fig. 11. Transmission PIP using the fundamental rotative modes in two waveguide sections containing an LTT 6301-2 ferrite rod surrounded by dielectric.

TABLE III

Type of Operation	Waveguide containing a L.T.T. 6301.2 ferrite rod surrounded by SiO_2 f = 9,5 GHz							
	a optimum (mm)	a/b optimum	b optimum (mm)	Δ β max (deg/cm)	α max (db/cm)	m (deg/db)	length for Δβ max =360° (cm)	insertion losses for Δβ max = 360° (db)
Positive mode	6	0,80	4,8	- 54,3	0,024	2 250	6,64	0,159
Negative mode	6	0,80	4,8	+157,8	0,025	6 250	2,28	0,057
Transmission P.I.P.	6	0,60	3,6	+ 96,5	0,038	2 445	3,73x2=7,46	0,143

Since $\tau_1 \neq \tau_2, \psi_1$ and ψ_2 must satisfy the wave equation

$$\nabla_T^2 \psi_{1,2} + s_1^2, {}_2 \psi_{1,2} = 0 \qquad \text{(A-4)}$$

we determine

$$\tau_{1,2} = \frac{s_{1,2}^2 - f}{g} = \frac{e}{s_{1,2}^2 - d}$$

from (A-3) and these relationships show that s_1^2 and s_2^2 are solutions of the quadratic equation

$$s^4 - (f + d)s^2 + fd - eg = 0 \qquad \text{(A-5)}$$

where $(fd - eg) \neq 0$ so that (A-5) has no confused roots. The calculation gives

$$fd - eg = \frac{\mu_z}{\mu} \beta_0^4 (\bar{k}_f^4 - \epsilon_f^2 K^2).$$

The condition $(fd - eg) \neq 0$ can thus be reduced to the condition

$$\bar{k}_f^4 - \epsilon_f^2 K^2 \neq 0$$

that is

$$\Gamma^2 \neq -\beta_0^2 \epsilon_f (\mu \pm k).$$

We recognize the values of the propagation constant for circularly polarized waves traveling in an unbounded ferrite medium.

These values being excluded, the solutions of (A-4) are expressed:

$$s_{1,2}^2 = \frac{f + d}{2} \pm \frac{1}{2} [(f - d)^2 + 4eg]^{1/2}. \qquad \text{(A-6)}$$

Let us develop (A-4) in cylindrical polar coordinates:

$$\left(\frac{\partial^2}{\partial_r^2} + \frac{1}{r} \frac{\partial}{\partial_r} + \frac{1}{r^2} \frac{\partial^2}{\partial \theta^2} + \frac{\partial}{\partial_z} \right) \psi_{1,2} + s_{1,2}^2 \psi_{1,2} = 0$$

and let us apply the separation method for variables by stating

$$\psi_{1,2}(r,\theta,z) = \psi_{1,2}(r)\psi_{1,2}(\theta)\psi_{1,2}(z).$$

This yields to

$$\psi_{1,2}(r) = J_n(s_{1,2} r) \text{ bounded at the origin}$$

$$\psi_{1,2}(\theta) = \exp(jn\theta)$$

$$\psi_{1,2}(z) = \exp(-\Gamma z)$$

where n is an integer positive or negative and $s_{1,2}$ are the radial wavenumbers.

APPENDIX II

EXPRESSION OF THE COMPLEX FIELDS IN THE FERRITE AND THE DIELECTRIC

The field components are assigned with the sign $-$ or $+$, according to whether they correspond to the left- or right-hand rotative mode.

1) In the Dielectric:

$$E_{zd}^{\mp}(r,\theta,z,t) = \pm [A_1 J_1(k_d r) + A_2 Y_1(k_d r)] \cdot \exp(\pm j\theta) \exp(-\Gamma z) \exp(j\omega t)$$

$$H_{zd}^{\mp}(r,\theta,z,t) = \pm [A_2 J_1(k_d r) + A_4 Y_1(k_d r)] \cdot \exp(\pm j\theta) \exp(-\Gamma z) \exp(j\omega t)$$

$$\boldsymbol{E}_{T_d}^{\mp} \begin{cases} E_{r_d}^{\mp} = -\dfrac{\beta_0}{k_d^2} \left[\bar{\Gamma} \dfrac{\partial E_{zd}^{\mp}}{\partial r} \mp \dfrac{\eta_0}{r} H_{z_d}^{\mp} \right] \\ E_{\theta_d}^{\mp} = j \dfrac{\beta_0}{k_d^2} \left[\eta_0 \dfrac{\partial H_{zd}^{\mp}}{\partial r} \mp \dfrac{\bar{\Gamma}}{r} E_{z_d}^{\mp} \right] \end{cases}$$

$$\boldsymbol{H}_{T_d}^{\mp} \begin{cases} H_{rd}^{\mp} = -\dfrac{\beta_0}{k_d^2} \left[\bar{\Gamma} \dfrac{\partial H_{zd}^{\mp}}{\partial r} \pm \dfrac{\epsilon_d}{\eta_0 r} E_{zd}^{\mp} \right] \\ H_{\theta_d}^{\mp} = j \dfrac{\beta_0}{k_d^2} \left[\dfrac{\epsilon_d}{\eta_0} \dfrac{\partial E_{zd}^{\mp}}{\partial r} \pm \dfrac{\bar{\Gamma}}{r} H_{z_d}^{\mp} \right]. \end{cases}$$

2) In the Magnetized Ferrite ($H_i > 0$):

Off the guide axis:

$$E_{z_f}^{\pm}(r,\theta,z,t) = \pm [A_5 J_1(s_1 r) + A_6 J_1(s_2 r)] \exp(\pm j\theta) \cdot \exp(-\Gamma z) \exp(j\omega t)$$

$$H_{z_f}^{\mp}(r,\theta,z,t) = \pm [A_5 \tau_1 J_1(s_1 r) + A_6 \tau_2 J_1(s_2 r)] \cdot \exp(\pm j\theta) \exp(-\Gamma z) \exp(j\omega t)$$

$$\boldsymbol{E}_{T_f}^{\mp} \begin{cases} E_{r_f}^{\mp} = \dfrac{1}{\beta_0(\epsilon_f^2 K^2 - \bar{k}_f^4)} \left[\bar{\Gamma} \left(\bar{k}_f^2 \dfrac{\partial E z_f^{\mp}}{\partial r} \mp \dfrac{\epsilon_f K}{r} E_{z_f}^{\mp} \right) - \eta_0 K \bar{\Gamma}^2 \dfrac{\partial H_{z_f}^{\mp}}{\partial r} \pm \eta_0 (\epsilon_f K^2 - \mu \bar{k}_f^2) \dfrac{H_{z_f}^{\mp}}{r} \right] \\ E_{\theta_f}^{\mp} = \dfrac{j}{\beta_0(\epsilon_f^2 K^2 - \bar{K}_f^4)} \left[\bar{\Gamma} \left(-\epsilon_f K \dfrac{\partial E_{z_f}^{\mp}}{\partial r} \pm \dfrac{\bar{K}_f^2}{r} E_{z_f}^{\pm} \right) + \eta_0 (\epsilon_f K^2 - \mu \bar{k}_f^2) \dfrac{\partial H_{z_f}^{\mp}}{\partial r} \mp \eta_0 K \dfrac{\bar{\Gamma}^2}{r} H_{z_f}^{\mp} \right] \end{cases}$$

$$\boldsymbol{H}_{Tf}^{\mp} \begin{cases} H_{r_f}^{\mp} = \dfrac{1}{\beta_0(\epsilon_f^2 K^2 - \bar{k}_f^4)} \left[\bar{\Gamma} \left(\bar{k}_f^2 \dfrac{\partial H_{z_f}^{\mp}}{\partial r} \mp \dfrac{\epsilon_f K}{r} H_{z_f}^{\pm} \right) - \dfrac{\epsilon_f}{\eta_0} \left(\epsilon_f K \dfrac{\partial E_{z_f}^{\mp}}{\partial r} \mp \dfrac{\bar{k}_f^2}{r} E_{z_f}^{\pm} \right) \right] \\ H_{\theta_f}^{\mp} = \dfrac{j}{\beta_0(\epsilon_f^2 K^2 - \bar{k}_f^4)} \left[\bar{\Gamma} \left(-\epsilon_f K \dfrac{\partial H_{z_f}^{\mp}}{\partial r} \pm \dfrac{\bar{k}_f^2}{r} H_{z_f}^{\pm} \right) + \dfrac{\epsilon_f}{\eta_0} \left(\bar{k}_f^2 \dfrac{\partial E_{z_f}^{\mp}}{\partial r} \mp \dfrac{\epsilon_f K}{r} E_{z_f}^{\pm} \right) \right]. \end{cases}$$

On the guide axis:

$$E_{z_f}^{\mp}(0,0,z,t) = H_{z_f}^{\mp}(0,0,z,t) = 0$$

$$\boldsymbol{E}_{T}^{\mp}{}_{f}\begin{cases} E_{xf}^{\pm}(0,0,z,t) = \dfrac{\exp(-\Gamma z)\exp(j\omega t)}{2\beta_0[\bar{\Gamma}^2+\epsilon_f(\mu\pm K)]} \cdot[[\eta_0(\mu\pm K)\tau_1 \mp \bar{\Gamma}]s_1A_5 + [\eta_0(\mu\pm K)\tau_2 \mp \bar{\Gamma}]s_2A_6] \\ E_{yf}^{\mp}(0,0,z,t) = \pm jE_{x_f}^{\mp}(0,0,z,t) \end{cases}$$

$$\boldsymbol{H}_{T_f}^{\mp}\begin{cases} H_{x_f}^{\mp}(0,0,z,t) = \dfrac{\exp(-\Gamma z)\exp(j\omega t)}{2\beta_0[\bar{\Gamma}^2+\epsilon_f(\mu\pm K)]} \cdot\left[\left(\dfrac{-\epsilon_f}{\eta_0}\mp\bar{\Gamma}\tau_1\right)s_1A_5 + \left(\dfrac{-\epsilon_f}{\eta_0}\mp\bar{\Gamma}\tau_2\right)s_2A_6\right] \\ H_{yf}^{\pm}(0,0,z,t) = \pm jH_{x_f}^{\mp}(0,0,z,t). \end{cases}$$

APPENDIX III

IN THE DEMAGNETIZED FERRITE ($H_i = 0$)

Off the guide axis:

$$E_{z_f}^{\mp}(r,\theta,z,t) = \pm A_5{}^iJ_1(k_f{}^ir)\exp(\pm j\theta)\exp(-\Gamma i_z)\cdot\exp(j\omega t)$$

$$H_{z_f}^{\mp}(r,\theta,z,t) = \pm A_6{}^iJ_1(k_f{}^ir)\exp(\pm j\theta)\exp(-\Gamma i_z)\cdot\exp(j\omega t)$$

$$\boldsymbol{E}_{T_f}^{\mp}\begin{cases} E_{r_f}^{\mp} = -\dfrac{\beta_0}{k_f{}^{i2}}\left[\bar{\Gamma}^i\dfrac{\partial E_{z_f}^{\mp}}{\partial r}\mp\eta_0\dfrac{\mu_i}{r}H_{z_f}^{\mp}\right] \\ E_{\theta_f}^{\mp} = \dfrac{j\beta_0}{k_f{}^{i2}}\left[\eta_0\mu_i\dfrac{\partial H_{z_f}^{\mp}}{\partial r}\mp\dfrac{\bar{\Gamma}^i}{r}E_{z_f}^{\mp}\right] \end{cases}$$

$$\boldsymbol{H}_{T_f}^{\mp}\begin{cases} H_{r_f}^{\mp} = -\dfrac{\beta_0}{k_f{}^{i2}}\left[\bar{\Gamma}^i\dfrac{\partial H_{z_f}^{\mp}}{\partial r}\pm\dfrac{\epsilon_f}{\eta_0 r}E_{z_f}^{\mp}\right] \\ H_{\theta_f}^{\mp} = -j\dfrac{\beta_0}{k_f{}^{i2}}\left[\dfrac{\epsilon_f}{\eta_0}\dfrac{\partial E_{z_f}^{\mp}}{\partial r}\pm\dfrac{\bar{\Gamma}^i}{r}H_{z_f}^{\mp}\right]. \end{cases}$$

On the guide axis:

$$E_{z_f}^{\mp}(0,0,z,t) = H_{z_f}^{\mp}(0,0,z,t) = 0$$

$$\boldsymbol{E}_{T_f}^{\mp}\begin{cases} E_{x_f}^{\mp}(0,0,z,t) = \dfrac{\beta_0}{2k_f{}^i}[\eta_0\mu_iA_6 \mp \bar{\Gamma}^iA_5] \cdot\exp(-\Gamma^iz)\exp(j\omega t) \\ E_{y_f}^{\mp}(0,0,z,t) = \pm jE_{d_f}^{\mp}(0,0,z,t) \end{cases}$$

$$\boldsymbol{H}_{T_f}^{\mp}\begin{cases} H_{x_f}^{\mp}(0,0,z,t) = \dfrac{\beta_0}{2k_f{}^i}\left[-\dfrac{\epsilon_f}{\eta_0}A_5 \mp \bar{\Gamma}^iA_6\right] \cdot\exp(-\Gamma^iz)\exp(j\omega t) \\ H_{y_f}^{\mp}(0,0,z,t) = \pm jH_{x_f}^{\mp}(0,0,z,t). \end{cases}$$

ACKNOWLEDGMENT

The authors wish to thank the team of analysts: M. Delfour, Mrs. Gimonet, and Miss de Robert for performing the numerical analysis part of this study.

REFERENCES

[1] M. L. Kales, "Modes in waveguide containing ferrites," *J. Appl. Phys.*, vol. 24, p. 1231, Jan. 1952.
[2] A. A. M. Vantrier, "Guided electromagnetic waves in anisotropic media," *Appl. Sci. Res.*, vol. 3, sect. B, pp. 305–371, 1953.
[3] R. A. Waldron, "Electromagnetic wave propagation in cylindrical waveguide containing gyromagnetic media," *J. Brit. Inst. Radio Eng.*, vol. 18, pp. 597–610, pp. 671–690, pp. 733–746, 1958.
[4] A. Delfour, A. Priou, and F. E. Gardiol, "A method for the determination of all the propagating modes in a loaded waveguide structure," presented at the IEEE G-MTT Int. Microwave Symp., Chicago, Ill., 1972.
[5] F. E. Gardiol, "Anisotropic slabs in rectangular waveguide," *IEEE Trans. Microwave Theory Tech.*, vol. MTT-18, pp. 461–466, Aug. 1970.
[6] S. R. Monaghan and M. C. Mohr, "Polarization insensitive phase shifter for use in phased-array antennas," *Microwave J.* Dec. 1969.
[7] C. R. Boyd, Jr., "A dual-mode latching reciprocal ferrite phase shifter," *IEEE Trans. Microwave Theory Tech. (1970 Symposium Issue)*, vol. MTT-18, pp. 1119–1124, Dec. 1970.
[8] N. B. Sultan, "Generalized theory of waveguide differential phase sections and application to novel ferrite devices," *IEEE Trans. Microwave Theory Tech.*, vol. MTT-19, pp. 348–357, Apr 1971
[9] J J. Green, "Microwave properties of partially magnetized ferrites," presented at the IEEE G-MTT Int. Microwave Symp., 1971.
[10] G. T. Rado, "Theory of the microwave permeability tensor and Faraday effect in non saturated ferromagnetic materials," *Phys. Rev.*, vol. 89, p. 529, 1953.
[11] A. M. Duputz and A. C. Priou, "TE_{11} circular waveguide ferrite phasers optimization," presented at the INTERMAG Conf., 1973.